Journal of Applied Physics | ARTICLE | scitation.org/journal/jap

# Do cities have a unique magnetic pulse?

Cite as: J. Appl. Phys. **131**, 204902 (2022); doi: 10.1063/5.0088264
Submitted: 15 February 2022 · Accepted: 23 April 2022 ·
Published Online: 31 May 2022

View Online Export Citation CrossMark

V. Dumont,[1,a)] T. A. Bowen,[2,3] R. Roglans,[2,3] G. Dobler,[4,5,6,7] M. S. Sharma,[7] A. Karpf,[8] S. D. Bale,[2,3] A. Wickenbrock,[9,10] E. Zhivun,[2] T. Kornack,[11] J. S. Wurtele,[2] and D. Budker[2,9,10]

## AFFILIATIONS

[1]Computational Research Division, Lawrence Berkeley National Laboratory, Berkeley, California 94720, USA
[2]Department of Physics, University of California, Berkeley, Berkeley, California 94720-7300, USA
[3]Space Sciences Laboratory, University of California, Berkeley, Berkeley, California 94720-7300, USA
[4]Biden School of Public Policy and Administration, University of Delaware, Newark, Delaware 19716, USA
[5]Department of Physics and Astronomy, University of Delaware, Newark, Delaware 19716, USA
[6]Data Science Institute, University of Delaware, Newark, Delaware 19713, USA
[7]Center for Urban Science and Progress, New York University, Brooklyn, New York 11201, USA
[8]Civil and Urban Engineering, Tandon School of Engineering, New York University, Brooklyn, New York 11201, USA
[9]Institut für Physik, Johannes Gutenberg-Universität Mainz, Staudingerweg 7, 55128 Mainz, Germany
[10]Helmholtz Institut Mainz, Staudingerweg 18, 55128 Mainz, Germany
[11]Twinleaf LLC, 300 Deer Creek Drive, Plainsboro, New Jersey 08536, USA

[a)]**Author to whom correspondence should be addressed:** vincentdumont11@gmail.com



## ABSTRACT

We present a comparative analysis of urban magnetic fields between two American cities: Berkeley (California) and Brooklyn Borough of New York City (New York). Our analysis uses data taken over a four-week period during which magnetic field data were continuously recorded using a fluxgate magnetometer with $70\,\mathrm{pT}/\sqrt{\mathrm{Hz}}$ noise. We identified significant differences in the magnetic signatures. In particular, we noticed that Berkeley reaches a near-zero magnetic field activity at night, whereas magnetic activity in Brooklyn continues during nighttime. We also present auxiliary measurements acquired using magnetoresistive vector magnetometers (VMRs), with the noise of $300\,\mathrm{pT}/\sqrt{\mathrm{Hz}}$, and demonstrate how cross correlation, and frequency-domain analysis, combined with data filtering can be used to extract urban-magnetometry signals and study local anthropogenic activities. Finally, we discuss the potential of using magnetometer networks to characterize the global magnetic field of cities and give directions for future development.



## I. INTRODUCTION

Cities are among the most complex systems that are of utmost importance for humanity. The multifaceted and dynamic properties of cities are determined by intricate combinations of natural, anthropogenic, and socio-economic factors. In recent years, a novel approach to the study of the cities was introduced,[1] in which a city is studied, similar to an astronomical object in the multi-messenger astronomy approach, with an array of observational instruments, such as, for example, multispectral cameras.[2–4] The analysis of such data has led to important insights into the working of cities,[5–7] of importance in such diverse areas as improving energy efficiency, reducing pollution, and increasing our understanding of social organization via the analysis of the work/sleep patterns of urban dwellers (with measurements carried out in a way to ensure privacy of individuals[8]).

With regard to the magnetic field in urban environments, studies have generally been limited to particular applications, such as health and safety[9] or geophysical prospection of archeological sites.[10,11] Motivated by the success of the multispectral approach, we built a prototype network for urban magnetometers[12] and conducted measurements in the San Francisco Bay Area, analyzing the dominant sources of magnetic signals and learning to extract subtle information in the presence of much larger backgrounds.

Here, we report the next step in the urban-magnetometry program, in which we compare the magnetic signatures of two cities, Berkeley (CA) and Brooklyn Borough of New York City (NY). Apart from the anticipated result that "New York never sleeps," our measurements indicate that each city has distinct magnetic signatures that can, perhaps, be exploited for the analysis of anomalies in city operation and long-term trends of the development of cities.

## II. EXPERIMENTAL DETAILS

### A. Sensor type and data acquisition

Two types of magnetometers were used to measure the magnetic field in Brooklyn. The base stations were built using eFM-3A three-axis fluxgate magnetometers manufactured by BioMed Jena GmbH.[13] These Biomed sensors are tied to a specific location and have a noise level of about 70 $pT/\sqrt{Hz}$.[14] We note that sensors that have lower noise may not be of much advantage for urban magnetometry because the environmental noise by far exceeds the sensor noise; see, for example, Fig. 1. A power supply from the same manufacturer is used to connect the magnetometers to a computer. Digitized magnetic field measurement data are transferred using a universal serial bus (USB) connection. The data streamed from the Biomed sensors are sampled at 3960 Hz and recorded on the computer using the publicly available UrbanMagnetometer software.[15] Data from each magnetic field direction (that is, X, Y, and Z) are stored hourly in separate binary files.

Field measurements were performed using magnetoresistive vector magnetometers (VMRs) manufactured by Twinleaf LLC with the noise at 1 Hz of 300 $pT/\sqrt{Hz}$.[16] In this work, we analyze the total scalar field and not individual vector measurements from each axes.[17] In terms of acquisition, the Twinleaf sensors do not require any data-acquisition device and can be powered directly from a laptop USB port, making them ideal for field measurements (see Sec. III C).

The geomagnetic field was acquired from the United States Geological Survey (USGS) using the open-source library Geomag Algorithms.[18] The USGS station (FRN) nearest to Berkeley is located 200 miles away, in Fresno, California. For the Brooklyn data, the nearest USGS station (FRD) is in Corbin, Virginia, about 300 miles away from New York City.

### B. Activity period

Data from the Biomed sensors were obtained over four weeks from each city during the calendar year 2016 for Berkeley and 2018 for Brooklyn. More specifically, the data used from Berkeley were taken from Monday, March 14, 2016, to Monday, April 11, 2016. The data from Brooklyn were acquired from Monday, May 7, 2018, to Monday, June 4, 2018; this period included the US Federal

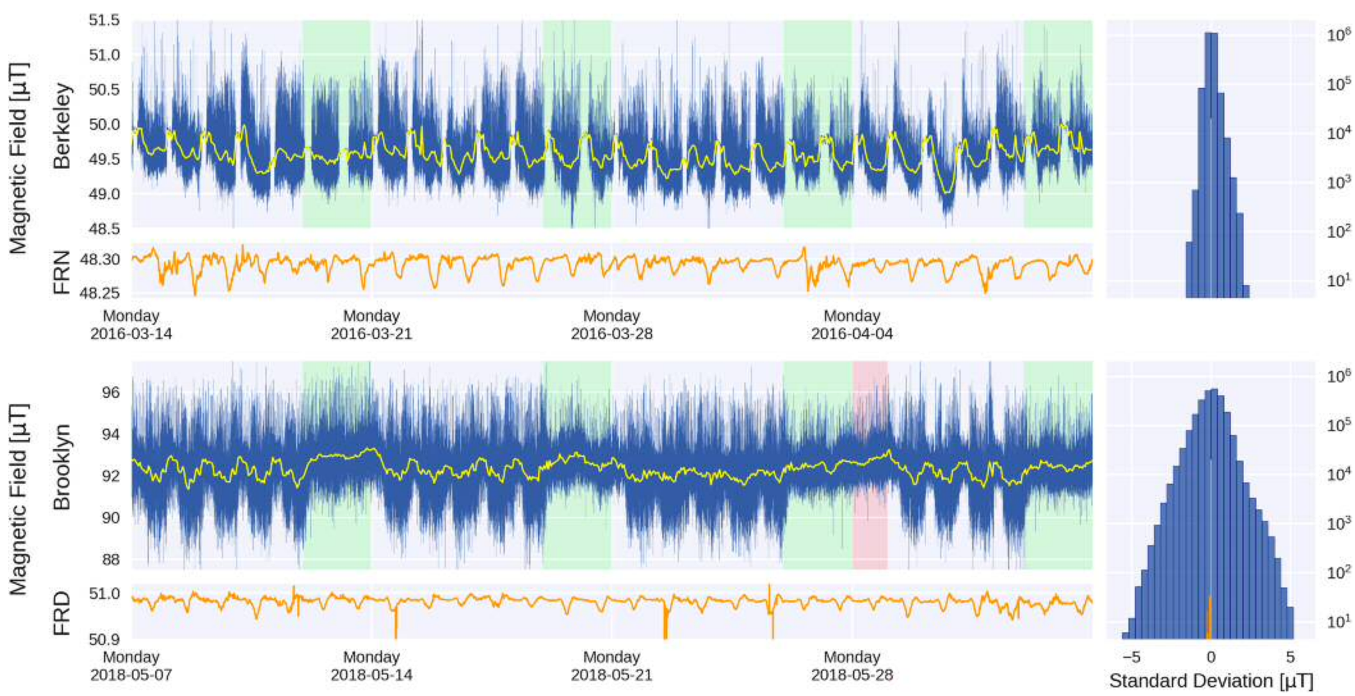


**FIG. 1.** Full four-week time series of urban magnetic field data for Berkeley (top) and Brooklyn (bottom). Data downsampled to 1 Hz are shown in blue, while the data in yellow represent the downsampled hour-rate time series. The weekends are highlighted by the light green regions and holiday (Memorial Day) in light red. We note the differences in vertical scales between both cities; in particular, the excursions of magnetic field are significantly larger in Brooklyn. The geomagnetic field taken from the closest USGS station is shown in orange. The relative variation of the magnetic field around its mean value is shown on the right hand side with the distribution from the geomagnetic field represented in orange.

Memorial Day holiday, observed the last Monday of the month (May 28, 2018), which is highlighted in red in Fig. 1. Holidays are usually characterized by a quieter magnetic environment due to a dropping off human activities; this can be particularly noticeable when the holiday falls on a weekday and the nearby environment surrounding the sensor has an overall magnetic field of higher amplitude during working hours.

Finally, an examination of the geomagnetic field measured by the respective USGS station closest to each city shows a decrease of 0.2 $\mu$T from the first measurement period in March 2016 to the second period in May 2018. This downward trend of the global geomagnetic field has been subject to several studies.[19,20] However, in the context of our work, the seasonal/annual variations of the natural magnetic background and its differences between the two locations are negligibly small and represent a small fraction of the urban variation studied in this work, i.e., 3% and below.

### C. Sensor locations

The Berkeley measurements (originally presented in Ref. 12) were conducted using geographically separated magnetometers in the city of Berkeley. The four-week data used in this work were generated by one of the Biomed sensors located in a residential area 90 m away from the Bay Area Rapid Transit (BART) rail system. The city of Berkeley has about 120 000 residents, living primarily in houses with a few low-rise buildings in the downtown. A BART line, which crosses the city, is the dominant source of magnetic field above the natural background during daytime.[21]

In Brooklyn, the Biomed sensor was placed on the 12th floor of the downtown-located Transit Building (370 Jay Street) in one of the corner offices of NYU's Center for Urban Science and Progress. In sharp contrast to Berkeley that has a population density of about 4600 people per square kilometer (2020 census), Brooklyn is over 3 times denser with a population density approaching 15 000 people per square kilometer, and its downtown constitutes a major transportation axis connecting it to downtown Manhattan. Located 40 m underneath the sensor's position, beneath the Transit Building, is the Jay Street-MetroTech subway station, which is served by three subway lines at all times and by several additional lines during commute hours.

Due to limited resources, we were only able to stream data seamlessly from one base station in Brooklyn, located in the Jay Street building. As the observations are limited to a single-point measurement from the building, the question arises as to whether or not these magnetic field fluctuations are characteristic of the magnetic environment of Brooklyn or, alternatively, if the fluctuations in the magnetic field are the result of a geographically localized set of magnetic sources in the Jay Street building. To address this concern, we performed a series of auxiliary experiments using multiple portable magnetic sensors (see Sec. III C) and demonstrate that while local processes measured by the Jay Street sensor are predominant, characteristic observations of the Brooklyn urban magnetic field can also be extracted from the data.

## III. COMPARATIVE DATA ANALYSIS

### A. Time-domain observations

The total scalar field for the entire four-week period for both cities is shown in Fig. 1. While daily variations of the magnetic field in Berkeley appear similar regardless of the day of the week (weekday fluctuations are similar to weekend fluctuations), the periodic behavior observed in the Brooklyn weekday data appears to stop on weekends and holidays. We note, however, that since the sensor in Brooklyn is placed within a business building, the drop in activities within the building during weekends and holidays (e.g., stopped elevators, lights off) represents a direct cause for the drop in magnetic field activities observed by the magnetometer. One should also note that the measured field is relatively far from the geomagnetic mean, indicating that the field on the sensor has a large contribution from a local source.

The change in variance during weekdays and weekends is shown on the top plots of Fig. 2. We note that the dispersion of the magnetic field in Berkeley is two orders of magnitude less at night than during the day, dropping from $10^{-2}$ to $10^{-4}\,\mu\text{T}^2$, while nightly variations in downtown Brooklyn remain high with a variance lying above $0.1\,\mu\text{T}^2$ all the time. Decreased amplitude fluctuations in Berkeley occur roughly between 1 and 4:30 a.m. when BART is not in service. We also note that nighttime activities differ slightly from weekday to weekend; this is a direct consequence of reduced public transport activities on weekends. In Brooklyn, however, the changes between daytime and nighttime variations are less pronounced and the weekend variation has only minor day/night variability. While a decrease in the anthropogenic activity during weekdays is usually observed at around 4–7 p.m., when business activities are reduced, the decrease in the magnetic field only starts to be seen at around 11 p.m., thereby suggesting that the magnetic field measured by the Biomed sensor is not solely driven by the occupancy of the building.

The bottom plots of Fig. 2 show the distributions of magnetic field data for the full dataset as well as for daytime and nighttime periods. For each city, day and nighttime distributions were fitted independently using a skewed Gaussian profile,

$$f(x; A, \mu, \sigma, \gamma) = \frac{A}{\sigma\sqrt{2\pi}} \exp\left[-(x-\mu)^2/(2\sigma^2)\right] \times \left\{1 + \text{erf}\left[\frac{\gamma(x-\mu)}{\sigma\sqrt{2}}\right]\right\}, \tag{1}$$

where $A$, $\mu$, $\sigma$, and $\gamma$ correspond, respectively, to the amplitude, mean, standard deviation, and skewness of the profile and erf[ ] is the error function. The best-fit results for each distribution are presented in Table I. Two observations can be made that distinguish the Berkeley magnetic field variations from Brooklyn. First, we note that while day and night time distributions recorded by the sensor in Brooklyn are centered around a consistent mean magnetic field of about 92.8 $\mu$T, the mean of both distributions in Berkeley is different with high significance, from a mean of 49.361(6) $\mu$T during the day to 49.925(9) $\mu$T at night. The second observation that can be made is the change in skewness of the distribution in Berkeley where the nighttime distribution profile sees an increase in

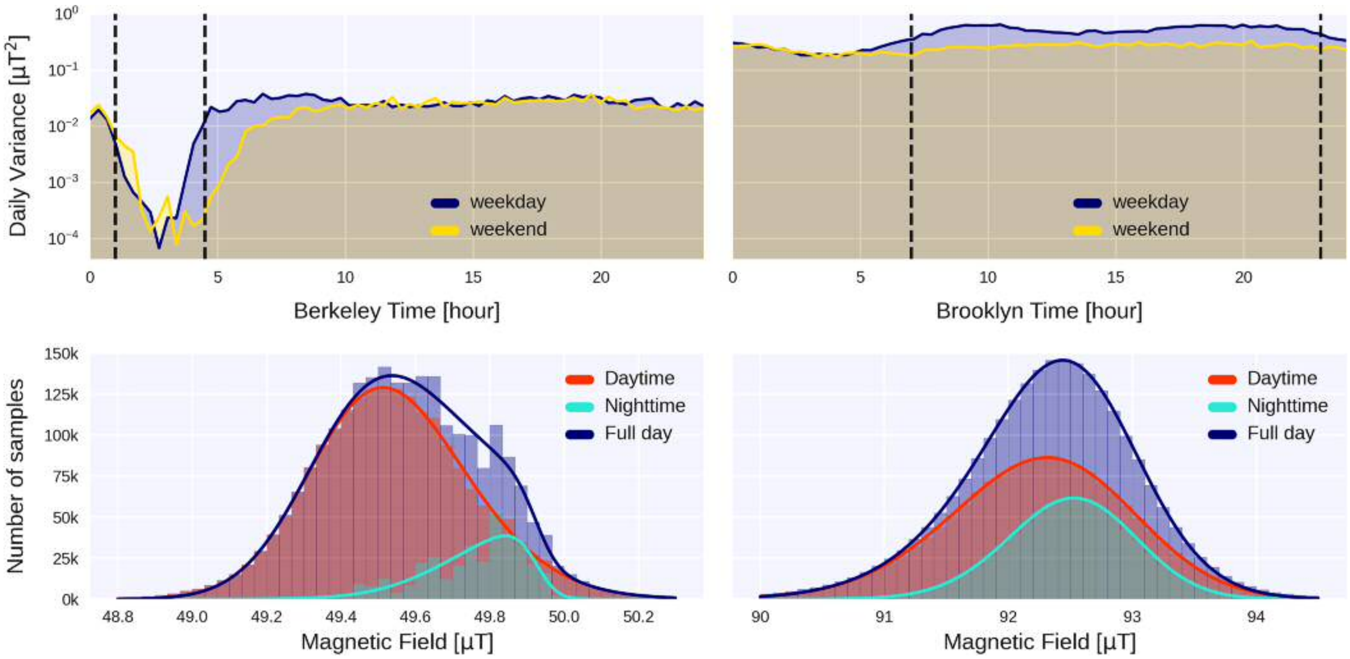


FIG. 2. Variance and distribution from Berkeley (left) and Brooklyn (right) data. The daily average variance was calculated over all the days for each consecutive 20 min time series. The vertical dashed lines on the top figures highlight the transition between day and night times. Nighttime has been set from 1 to 4:30 a.m. for Berkeley and 11 p.m. to 7 a.m. for Brooklyn. The bottom plots show the daytime (red) and nighttime (green) distributions as well as for the full day (blue). A skewed Gaussian was fitted to both daytime and nighttime histograms independently (see Table I for best-fit results). The blue skewed Gaussian profiles represent the sum of both daytime and nighttime profiles.

skewness compared with daytime variations. In Brooklyn, on the other hand, the distribution remains roughly Gaussian all the time with a low absolute skewness of around 1.

## B. Frequency content

In Fig. 3, we show the power spectral density (PSD) at high-frequency for both Berkeley and Brooklyn data. The drop in magnetic field activities in Berkeley at nighttime, identified in the variance plot (see top panels from Fig. 2), can be explained by the decrease in low-frequency signals (up to 10 Hz) in the PSD. We also note a significant difference in amplitude of the power line and other high-frequency signals between both cities (see bottom panels from Fig. 3).

TABLE I. Best skewed Gaussian fit of daytime and nighttime magnetic field distributions for Berkeley and Brooklyn data.

| | Berkeley | | Brooklyn | |
|---|---|---|---|---|
| Params | Daytime | Nighttime | Daytime | Nighttime |
| $A$ | 67 980(407) | 11 488(654) | 158 547(504) | 79 559(321) |
| $\mu$ ($\mu$T) | 49.361(6) | 49.925(9) | 92.802(14) | 92.833(18) |
| $\sigma$ ($\mu$T) | 0.281(5) | 0.212(18) | 0.930(12) | 0.617(12) |
| $\gamma$ | 1.39(8) | −4.61(148) | −1.15(5) | −0.93(7) |

Low-frequency signals for both daytime and nighttime periods are shown in Fig. 4. We notice that a 20 min signal at $8.3 \times 10^{-4}$ Hz is observed during daytime in Berkeley, which is known to be associated with the BART activities.[12] In Brooklyn, a similar signal is also observed, but at nighttime. In order to identify this 20 min periodic signal in the time-series data, we made 100 min averages of the daytime Berkeley and nighttime Brooklyn data. Applying a high-pass filter with a cutoff frequency at 0.001 Hz allows us to improve the extraction and visibility of the 20 min periodic signal (see bottom panels in Fig. 4). While the signal is already visible in the average 100 min data for Berkeley, the noise in the unfiltered data from Brooklyn provides greater challenges to identifying the 20 min signal.

In Fig. 5, we show a scalogram that demonstrates the richness of urban magnetic field data. The quiet nighttime perturbations in Berkeley, previously shown in Ref. 12, are recovered. Using the full-rate data, one can see how high-frequency ranges are richer in anthropogenic activities. In particular, irregular signals below the power frequency can often be seen and are more prominently in the Berkeley data.

## C. Auxiliary field measurements

The measurements previously made in Berkeley[12] revealed coherent magnetic field fluctuations in a geographically distributed magnetometer array. The significant correlations between stations

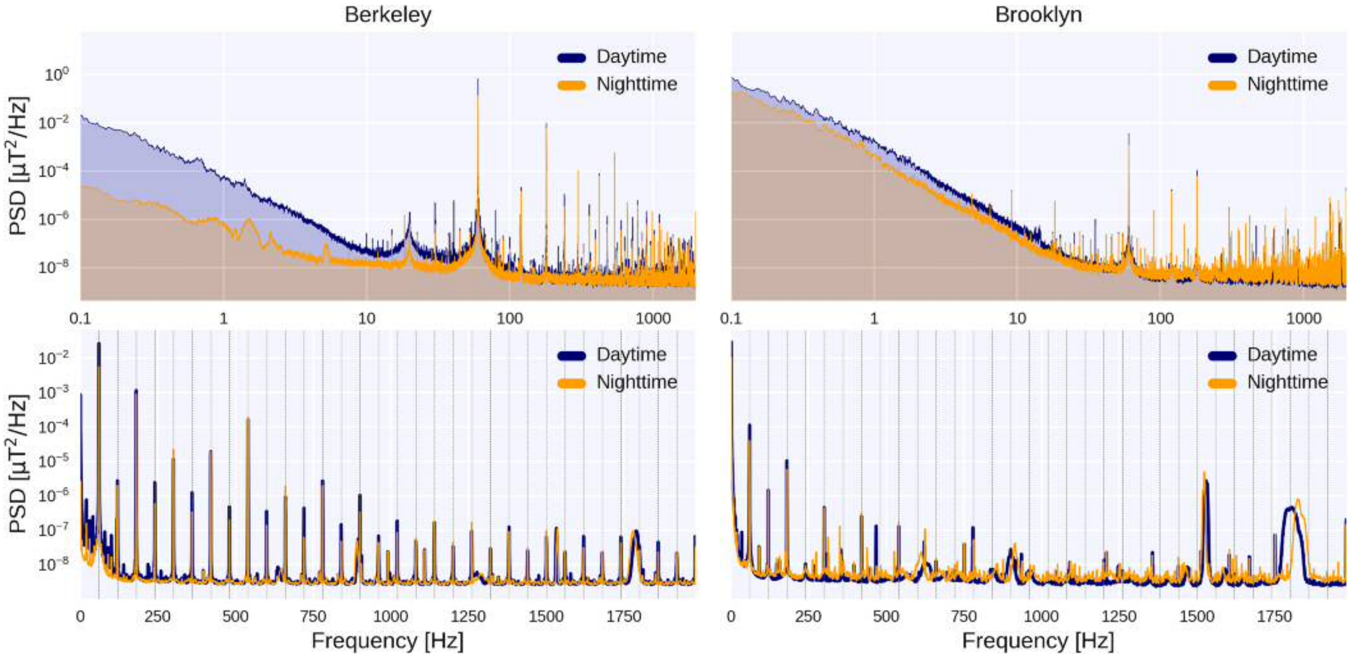


**FIG. 3.** High-frequency power spectral density (PSD) from Berkeley (left) and Brooklyn (right) in both logarithmic (top) and linear (bottom) scales. The PSDs were produced using the full-rate data, sampled at 3960 Hz. The 60 Hz power line and its harmonics can be seen clearly in the linear-scale PSD (bottom panel) and are highlighted by the thin dashed vertical lines.

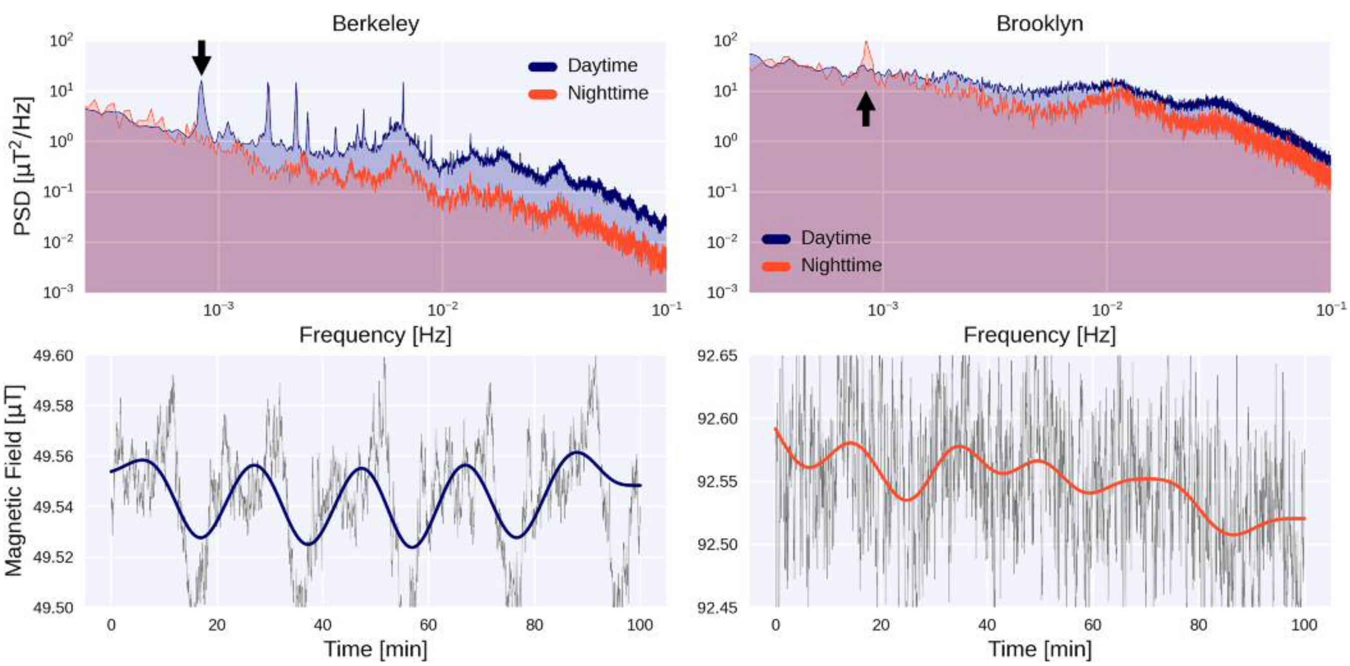


**FIG. 4.** Low-frequency PSDs with 20 min signal extraction. The top panels show the logarithmic-scale PSDs produced using decimated data at 1 Hz. The black arrows show a 20 min periodic signal ($8.3 \times 10^{-4}$ Hz) that can be found in the daytime variation from the Berkeley data and nighttime variations in Brooklyn. The bottom panels show the 20 min periodic signal extracted from an ensemble average of 100 min data regions after applying a high-pass filter with a cutoff frequency at 0.001 Hz.

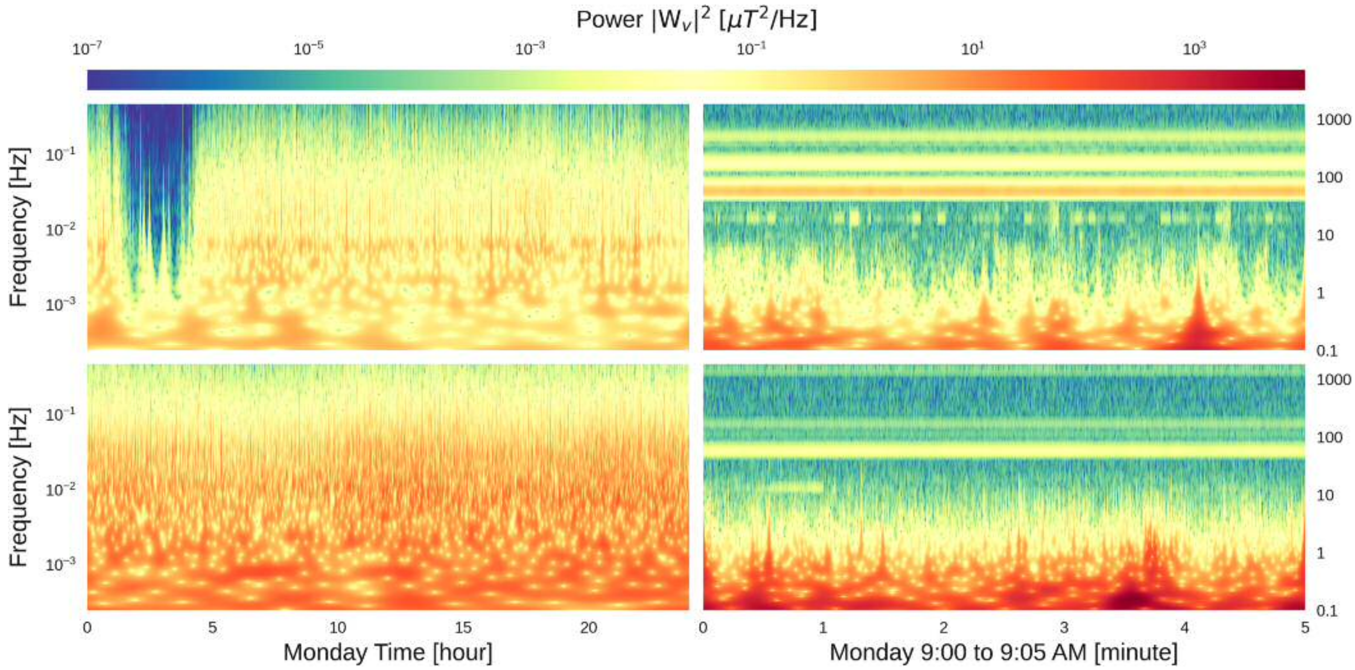


**FIG. 5.** Wavelet scalogram for a full day (left) and 5 min of data (right) for the first day (Monday) of both Berkeley (top) and Brooklyn (bottom) datasets. The full-day scalogram was achieved using the downsampled 1 Hz data and plotted from the lowest available frequency, i.e., inverse of sampling rate to 500 mHz. The 5 min scalograms were, on the other hand, produced using the full-rate data, thereby showing frequency content up to the Nyquist limit, i.e., half the sampling rate.

allowed identification of these fluctuations with a "global" magnetic field, which characterizes the magnetic signature of the city of Berkeley (or, rather, the broader East Bay). Therefore, in order to fully determine the signature of Brooklyn, or of New York City (NYC) at large, a comparative analysis of *in situ* data taken from two different environments must be made.

In Fig. 6, we show the behavior of the magnetic field in five distinct locations throughout Brooklyn. Each measurement was acquired using magnetoresistive vector magnetometers manufactured by Twinleaf LLC with data sampled at 200 Hz and the noise level as low as 300 pT/$\sqrt{\text{Hz}}$ at 1 Hz. As one can notice, downtown Brooklyn is an urban environment with a high diversity of magnetic field sources (e.g., elevators moving in buildings, cars on surface streets, subways crossing the Manhattan Bridge), thereby making the identification of a more global magnetic signature more challenging.

All field measurements were acquired using two stations to allow cross correlation between both instruments. Figure 7 demonstrates how challenging the cross correlation between individual stations that are geographically separated can be. While two stations placed close to each other (i.e., within a few meters, see the first column) hold highly cross-correlated data, the information quickly becomes uncorrelated the further away one station is from another.

However, using low-pass filters, it becomes possible to correlate signals from different environments. For instance, in the second column of Fig. 7, we cross correlate the magnetic field recorded from the sidewalk in front of the Jay Street building with the magnetic field recorded from inside the twelfth floor of the Jay Street building and identified a correlated signal with a lag time of 5 min between both stations. Similarly, when recording the magnetic field from the inside of two buildings located across the street from each other (see the last column in Fig. 7), a noticeable anti-correlated behavior can be observed.

## IV. DISCUSSION

### A. Optimal sensor network distributions

This work represents an initial demonstration of the potential complexity in small-scale magnetic field variability in dense urban environments. Indeed, in the context of the "magnetic field of a city," our observations show that the power in high spatial frequency modes is larger in a dense city like Brooklyn; this may be a feature of larger cities with a wider variety of magnetic sources. Small-spatial-scale effects must, therefore, be considered when designing optimal sensor network systems so they can map out the spatial variability of magnetic field on multiple scales.

### B. Impact of small-scale effects on global field

In this work, we attempt to characterize the global magnetic field of cities, that is, the portion of the magnetic field that has spatial and temporal variation, but is observed to have spatiotemporal correlations over the extent of the city system. A global magnetic system can be defined as the set of extended and point

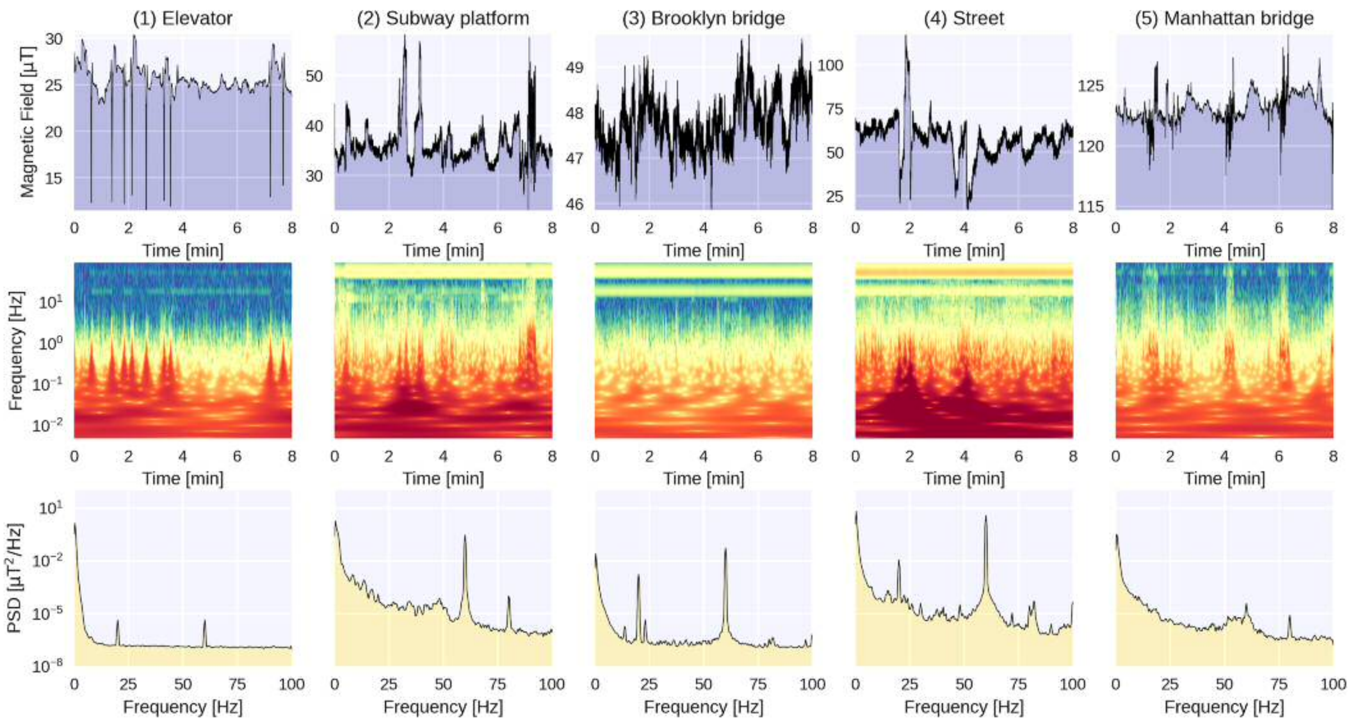


**FIG. 6.** Five samples of magnetic field time series at five different locations in Brooklyn. From left to right: (1) Elevator measurements were taken on the twelfth floor of Transit Building, (2) subway measurements were acquired from the Jay Street Metro Tech station, (3) Brooklyn bridge measurements were taken underneath the bridge, (4) street measurements were obtained on the sidewalk in front of the Transit Building in downtown Brooklyn, and (5) the Manhattan Bridge measurements were taken on top of the bridge from the middle of the walkway.



sources that contribute non-negligibly to its magnetic field. In the case of a city system, this often contains multiple subsystems, such as individual buildings and trains.

A subsystem generally contains a geographically localized (within a volume) set of magnetic sources, which are both extended and point-like in nature. For instance, building-specific fluctuations represent subsystems within larger systems where the time dependence includes effects from both the structure itself and the behavioral signals from the population that is using the structure. In our work, the base station located within the Jay Street building is subject to fields due to sources with a spatial extent comparable to that of the building, as well as any point sources within its subsystem. Presumably, the field measured with a sensor in the building can also have contributions from other subsystems, such as trains, for example, from the subway station underneath the Jay Street building.

Spatial and temporal variations in the magnetic field are often observed in the data and can be due to a variety of reasons, including the motion of magnetized objects or time variations in the current generating the magnetic field. While not all point sources, that is, sources confined to a certain small volume, have their magnetic field measurable beyond the vicinity of a few nearby sensors, these sources come with some characteristic radial dependence that perturb the larger spatial scale magnetic field, thereby making the extraction of the underlying global city-system field more challenging to perform.

### C. Inferring global properties from local measurements

Local measurements in a dense urban environment may have periodicities similar to the daily/weekly trends observed in all urban systems, and one could probably argue that the subsystems are coupled to these large-scale systems. However, periodicities in the global field (e.g., the extended urban environment) are harder to measure.

We further point out that point-source perturbations can be used to understand buildings in a global field but from an *in situ* experimental standpoint. However, it is hard to constrain any dynamics using a point-source assumption and a small number of sensors. Our interpretation of "subsystem" urban magnetic fields (i.e., local fluctuations) is that they basically consist of multiple dipoles (or multipoles) moving in potentially complex ways. A single sensor (even with vector measurements) is unable to uniquely determine a dipole moment/orientation. A minimum of two sensors is, therefore, needed; the same is true for fields generated by line current. An added challenge in understanding the variation of a localized source using a few measurement sites comes

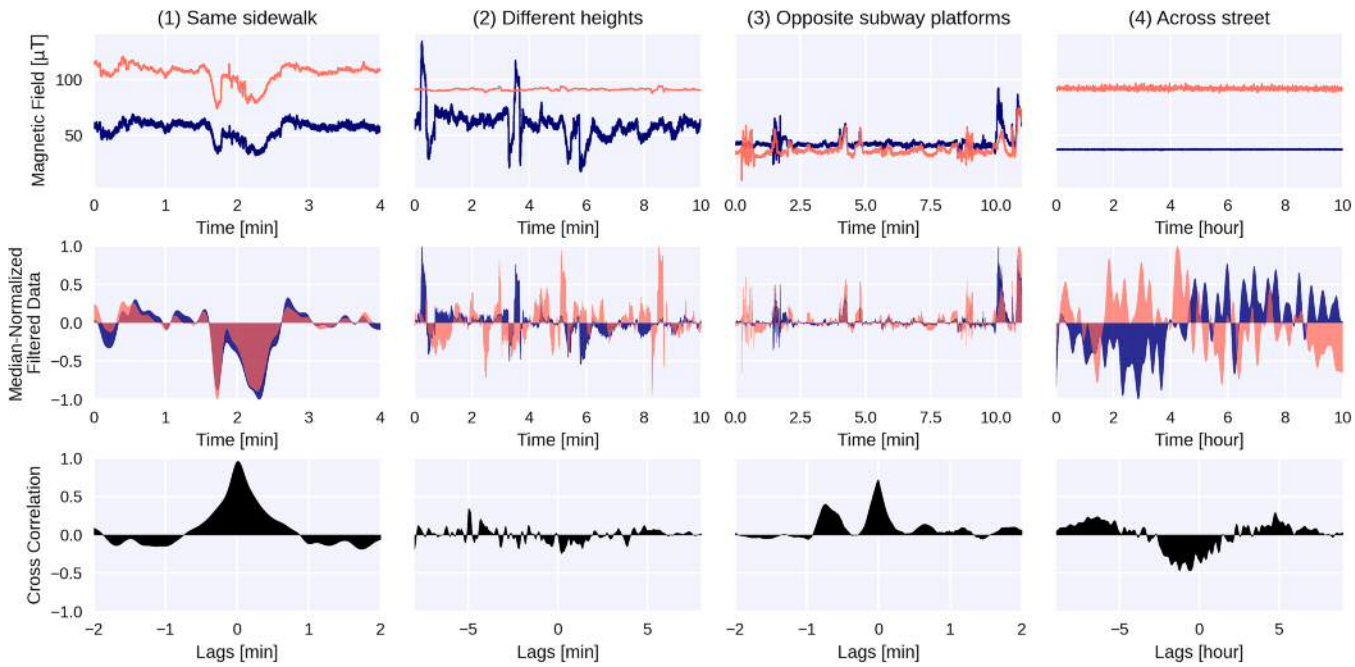


**FIG. 7.** Cross-correlated data between two sensors. (1) Sensors placed 7 m apart from each other on the sidewalk; a low-pass filter with a cutoff frequency at 0.1 Hz was applied to the data; (2) First sensor (blue) placed on the sidewalk and the second sensor (red) in the CUSP office on the 12th floor, low-pass filter applied with a cutoff frequency at 10 Hz; (3) sensors placed at opposite ends of one of the platforms in the Jay Street-MetroTech subway station, low-pass filter applied with a cutoff frequency at 10 Hz; (4) asynchronous measurements from 10 a.m. to 8 p.m., one recorded data (blue) were streamed from the old CUSP office at One MetroTech Center on Monday, October 9, 2017, while the second set of measurements (red) was made from across the street in the Transit Building on Monday, October 10, 2017, low-pass filter applied with a cutoff frequency at 0.001 Hz masking periodicity with timescale less than 16.7 min.



from the time dependence of the signals. Further investigations will need to address to what extent localized fields can, in practice, be isolated and identified using a magnetometer network.

The magnetic environment within a subsystem may be highly chaotic. A determination of the large-scale field properties from local measurements requires an analysis of the statistical variability in the measurements. An exception to a purely statistical approach might be when there is a single dominant source in the local subsystem, which can be subtracted from the local field.

## V. CONCLUSION

In this pilot study, magnetic signatures obtained in different urban environments (Berkeley and Brooklyn) were compared. We find that there are major differences in magnetic signatures in these two test cases, for example, the difference in the contrast of magnetic signatures between daytime and nighttime.

There are many ways to analyze the rich urban magnetic data. As we have shown in this work, some of them allow reducing the complex data stream to a few key parameters that can be used to monitor the dynamics of the city.

The results of this work point toward a number of possible future directions. For example, this is an extension to sensor networks as introduced in Ref. 12 and correlation with other (nonmagnetic) data, for instance, those from multispectral cameras.[4,5]

A specific advantage of magnetometry for urban studies is that it can provide information on the functioning of infrastructure within its boundaries, but at a distance (e.g., a moving elevator or operating machinery within a building that can be detected from the outside); therefore, uses might include post-disaster assessment (e.g., vulnerability of partially destroyed buildings), infrastructure monitoring (e.g., assessment of sensorless bridges with short bursts of observations), monitoring the stability of the power grid (with instabilities being precursors of outages), monitoring climate and weather events (e.g., detection of correlated lightning strike signatures), etc.

Some interesting multidisciplinary questions one could address include: How does an anomalous event, such as epidemic or pandemic, affect the urban magnetic signature? Are there significant monthly and/or seasonal variations of magnetic signatures? What are the origins of these variations? Are they the same for different cities?, etc. It is the authors' belief that answering these questions of "comparative urban magnetometry" will teach us a lot about cities, and this knowledge will eventually translate into tangible economic and social benefits.

There are also technical improvements that can benefit future urban-magnetometry studies. For example, if a measurement is done near a local source, vibrations of the sensor can lead to spurious signals. These, however, can be identified by correlating the magnetic readout with accelerometer data. In fact, the Twinleaf magnetometers that we used are already equipped with such auxiliary sensors.

## AUTHOR DECLARATIONS

### Conflict of Interest

The authors have no conflicts to disclose.

## DATA AVAILABILITY

The entirety of the data and codes used in this work have been made publicly available. Detailed instructions on how to access the data and reproduce the results presented here can be found in the online documentation accessible at http://citymag.gitlab.io/nuri/paper. The analysis was performed on 86 GB worth of magnetic field data using the open-source software NURI,[22] specifically designed to analyze time-series data produced by our urban-magnetometry network.

## REFERENCES


1. G. Dobler, M. Ghandehari, S. E. Koonin, R. Nazari, A. Patrinos, M. S. Sharma, A. Tafvizi, H. T. Vo, and J. S. Wurtele, "Dynamics of the urban lightscape," Inf. Syst. **54**, 115–126 (2015).
2. V. Lebourgeois, A. Bégué, S. Labbé, B. Mallavan, L. Prévot, and B. Roux, "Can commercial digital cameras be used as multispectral sensors? A crop monitoring test," Sensors **8**, 7300–7322 (2008).
3. H. Park and K. B. Crozier, "Multispectral imaging with vertical silicon nanowires," Sci. Rep. **3**, 1703 (2013).
4. L. Duempelmann, B. Gallinet, and L. Novotny, "Multispectral imaging with tunable plasmonic filters," ACS Photonics **4**, 236–241 (2017).
5. G. Dobler, M. Ghandehari, S. E. Koonin, and M. S. Sharma, "A hyperspectral survey of New York City lighting technology," Sensors **16**, 2047 (2016).
6. G. Dobler, F. B. Bianco, M. S. Sharma, A. Karpf, J. Baur, M. Ghandehari, J. Wurtele, and S. E. Koonin, "The urban observatory: A multi-modal imaging platform for the study of dynamics in complex urban systems," Remote Sens. **13**, 1426 (2021).
7. F. Qamar and G. Dobler, "Pixel-wise classification of high-resolution ground-based urban hyperspectral images with convolutional neural networks," Remote Sens. **12**, 2540 (2020).
8. C. E. Kontokosta, "Urban informatics in the science and practice of planning," J. Plan. Educ. Res. **41**, 382–395 (2021).
9. M. Lindgren, M. Gustavsson, Y. Hamnerius, and S. Galt, "Mapping of magnetic fields in city environment," in *Electricity and Magnetism in Biology and Medicine*, edited by F. Bersani (Springer US, Boston, MA, 1999), pp. 821–824.
10. J. Fassbinder, H. Becker, and M. van Ess, "Magnetometry at Uruk (Iraq): The city of king Gilgamesh," in *EGS–AGU–EUG Joint Assembly* (European Geophysical Society, 2003), p. 9152.
11. H. Becker, *Caesium-Magnetometry for Landscape-Archaeology* (CRC Press, 2008), pp. 129–165.
12. T. A. Bowen, E. Zhivun, A. Wickenbrock, V. Dumont, S. D. Bale, C. Pankow, G. Dobler, J. S. Wurtele, and D. Budker, "A network of magnetometers for multi-scale urban science and informatics," Geosci. Instrum. Methods Data Syst. **8**, 129–138 (2019).
13. More details on the characteristics of the Biomed's eFM-3A sensor can be found at http://citymag.gitlab.io/nuri/biomed.html.
14. The noise of the magnetometer is specified at 10 Hz. The $1/f$ knee for these devices[12] is at around 1 Hz.
15. L. Zhivun and V. Dumont, UrbanMagnetometer version 1.0.0, 2018.
16. See https://twinleaf.com/vector/VMR/ for VMR Magnetoresistive Vector Magnetometer.
17. There may be a small systematic effect in these measurements: The VMR sensors are based on HMC1001 series sensors and have variation over time and temperature such that the calibration of each axes can be off by as much as 10%, which may cause the recorded "scalar" measurements to not be purely scalar.
18. See https://github.com/usgs/geomag-algorithms for Geomag Algorithms.
19. P. Alken, E. Thébault, C. D. Beggan, H. Amit, J. Aubert, J. Baerenzung, T. N. Bondar, W. J. Brown, S. Califf, A. Chambodut, A. Chulliat, G. A. Cox, C. C. Finlay, A. Fournier, N. Gillet, A. Grayver, M. D. Hammer, M. Holschneider, L. Huder, G. Hulot, T. Jager, C. Kloss, M. Korte, W. Kuang, A. Kuvshinov, B. Langlais, J.-M. Léger, V. Lesur, P. W. Livermore, F. J. Lowes, S. Macmillan, W. Magnes, M. Mandea, S. Marsal, J. Matzka, M. C. Metman, T. Minami, A. Morschhauser, J. E. Mound, M. Nair, S. Nakano, N. Olsen, F. J. Pavón-Carrasco, V. G. Petrov, G. Ropp, M. Rother, T. J. Sabaka, S. Sanchez, D. Saturnino, N. R. Schnepf, X. Shen, C. Stolle, A. Tangborn, L. Tøffner-Clausen, H. Toh, J. M. Torta, J. Varner, F. Vervelidou, P. Vigneron, I. Wardinski, J. Wicht, A. Woods, Y. Yang, Z. Zeren, and B. Zhou, "International geomagnetic reference field: The thirteenth generation," Earth Planets Space **73**, 279 (2021).
20. C. Constable and M. Korte, "Centennial- to millennial-scale geomagnetic field variations," in *Treatise on Geophysics*, 2nd ed., edited by G. Schubert (Elsevier, Oxford, 2015), pp. 309–341.
21. A. C. Fraser-Smith and D. B. Coates, "Large-amplitude ULF electromagnetic fields from BART," Radio Sci. **13**, 661–668 (1978).
22. V. Dumont, NURI version 1.0.0, 2022.